KeAi

CHINESE ROOTS
GLOBAL IMPACT

Contents lists available at ScienceDirect

Petroleum Science

journal homepage: www.keaipublishing.com/en/journals/petroleum-science



Original Paper

Transportation and sealing pattern of the temporary plugging ball at the spiral perforation in the horizontal well section



Qing-Hai Hu ^a, Wan Cheng ^{a, *}, Zun-Cha Wang ^a, Yu-Zhao Shi ^a, Guang-Liang Jia ^b

- ^a Faculty of Engineering, China University of Geosciences, Wuhan, 430074, Hubei, China
- ^b Sinopec North China Oilfield Service Corporation, Zhengzhou, 445007, Henan, China

ARTICLE INFO

Article history: Received 18 February 2024 Received in revised form 18 June 2024 Accepted 24 June 2024 Available online 26 June 2024

Edited by Yan-Hua Sun

Keywords:
Temporary plugging ball
Horizontal well
Multistage fracturing
Spiral perforation
Numerical simulation

ABSTRACT

Multistage fracturing of horizontal wells is a critical technology for unconventional oil and gas reservoir stimulation. Ball-throwing temporary plugging fracturing is a new method for realizing uniform fracturing along horizontal wells and plays an important role in increasing oil and gas production. However, the transportation and sealing law of temporary plugging balls (TPBs) in the perforation section of horizontal wells is still unclear. Using COMSOL computational fluid dynamics and a particle tracking module, we simulate the transportation process of TPBs in a horizontal wellbore and analyse the effects of the ball density, ball diameter, ball number, fracturing fluid injection rate, and viscosity on the plugging efficiency of TPB transportation. This study reveals that when the density of TPBs is close to that of the fracturing fluid and a moderate diameter of the TPB is used, the plugging efficiency can be substantially enhanced. The plugging efficiency is greater when the TPB number is close to twice the number of perforations and is lower when the number of TPBs is three times the number of perforations. Adjusting the fracturing fluid injection rate from low to high can control the position of the TPBs, improving plugging efficiency. As the viscosity of the fracturing fluid increases, the plugging efficiency of the perforations decreases near the borehole heel and increases near the borehole toe. In contrast, the plugging efficiency of the central perforation is almost unaffected by the fracturing fluid viscosity. This study can serve as a valuable reference for establishing the parameters for temporary plugging and fracturing.

© 2024 The Authors. Publishing services by Elsevier B.V. on behalf of KeAi Communications Co. Ltd. This is an open access article under the CC BY-NC-ND license (http://creativecommons.org/licenses/by-nc-nd/

4.0/).

1. Introduction

Multistage fracturing of horizontal wells is an important production enhancement technique in the development of unconventional oil and gas reservoirs (Seale et al., 2006; Zeng et al., 2015). Due to the in-situ stress complexity and stress interference phenomenon among hydraulic fractures, some hydraulic fractures are short and narrow, which leads to insufficient oil and gas production (Olson, 2008; Roussel and Mukul, 2011; Zhao et al., 2016; Cheng et al., 2019). In the hydraulic fracturing of horizontal wells, the temporary plugging technique has been widely used to achieve uniform fracture expansion (Wang et al., 2012; Xiong et al., 2018a; Zhao et al., 2020; Zhou et al., 2022). By injecting fracturing fluid containing temporary plugging balls (TPBs), the TPBs will transport

along the wellbore, and some of the TPBs will sit on the perforation to form temporary plugs, inhibiting the expansion of the dominant fractures and guiding the secondary expansion of the short fractures (Xiong et al., 2018b; Zhang et al., 2020). However, the transportation and sealing laws of TPBs have not been fully understood. The throwing of TPBs in engineering practice relies mainly on personal experience, and its efficiency is low and randomized. Therefore, it is urgent to study the transportation and sealing law of TPBs in horizontal wellbores.

To date, many experts have conducted various types of research on TPB transportation in wellbores. Erbstoesser (1980) experimentally simulated buoyant TPB-blocking perforations for fracturing fluid diversion to realize multifracture expansion. Baylocq et al. (1999) proposed a design method for nonbuoyant ball temporary plugging for hydraulic fracturing diversion, and the positive impact enables the technology to be utilized in horizontal and inclined wells at a reasonable expense. Nozaki et al. (2013) conducted a series of full-scale experiments to assess the plugging efficiency of

E-mail address: Chengwancup@163.com (W. Cheng).

^{*} Corresponding author.

TPBs and analysed how many perforations were blocked in an acidfracturing field. Oberhofer (2016) proposed that the use of degradable balls to achieve temporary plugging can improve fracturing efficiency. Zhu et al. (2021) developed a degradable preformed particle gel, which has a good plugging effect. Li et al. (2020) and Zou et al. (2020) investigated the fracture expansion of temporary plugging segmental fractures via numerical simulation and verified the effectiveness of ball-throwing temporary plugging for fracturing. Cheng et al. (2021) analysed the forces of TPB transporting and seating. Brown et al. (1963) investigated the most important factors affecting the sealing performance of TPBs in vertical wells, which provided a basis for the design of temporary plugging processes. Marchioli et al. (2007) studied the effects of gravity and lift on the particle transport velocity in vertical wells. Li et al. (2005) proposed a complete transport model of the TPBs, providing a theoretical basis for their migration in a wellbore. Li (2017) conducted a series of experiments to simulate the sealing law of TPBs on perforation boreholes, but these authors studied only the sealing of perforations in a vertical well. Rong and Xu (2020) used computational fluid dynamics and the discrete element method (DEM) to investigate the mechanism of TPB transport and sealing in the horizontal well. In their study, the spatial distribution of TPBs in casings was determined, providing a meaningful insight into the transportation and sealing of TPBs in horizontal wellbores (Rong and Xu, 2020). However, his research on the influencing factors of TPB transportation and sealing effects is insufficient.

In this paper, the COMSOL computational fluid dynamics and a particle tracking module are used to establish a horizontal wellbore model with spiral perforations and to reveal the transportation trajectory and sealing law of a plugging ball. Through the single-variable method, we analyse the laws of movement and sealing of TPBs and identify five major influencing factors that determine plugging efficiency. This study provides theoretical and technical support for parameter optimization of the ball-throwing plugging fracturing technique in horizontal wells.

2. Numerical model

The transportation of TPB inside a horizontal wellbore is a typical two-phase particle flow problem that involves several physical processes. These processes include fluid flow inside the wellbore, movement of the TPB inside the fluid and interactions between them.

The fracturing fluid can be considered an incompressible Newtonian fluid and a homogeneous continuous medium. The equations of fluid motion are based on the continuous medium assumption and use the Navier—Stokes equations to describe the motion of the fluid (Norouzi et al., 2016; Barboza et al., 2021; Qu et al., 2023).

$$\begin{cases} \frac{\partial}{\partial t} \left(\alpha \rho_{\rm f} \right) + \nabla \left(\alpha \rho_{\rm f} \nu_{\rm f} \right) = 0 \\ \frac{\partial}{\partial t} \left(\alpha \rho_{\rm f} \nu_{\rm f} \right) + \nabla \left(\alpha \rho_{\rm f} \nu_{\rm f} \right) = -\alpha \nabla p + \nabla (\alpha \tau) + \alpha \rho_{\rm f} g + S_{\rm f} \end{cases}$$
(1)

where t is the time, s; α is the solid-phase volume fraction; ρ_f is the liquid density, kg/m^3 ; v_f is the liquid flow rate, m/s; p is the fluid pressure, Pa; τ is the viscous stress, Pa; g is the gravitational acceleration, m/s^2 ; and S_f is the source term of the momentum exchange between the fluid and the particles, N/m^3 .

The solid-phase volume fraction (Li et al., 2009) is calculated as

$$\alpha = 1 - \sum_{i=1}^{N} V_{b,i} / V_{\text{cell}}$$
 (2)

where *N* is the number of TPBs; $V_{b,i}$ is the volume of the *i*th TPB, m^3 ; and V_{cell} is the volume of the calculation cell, m^3 .

The source term of momentum exchange between the fluid and the TPB is given by

$$S_{\rm f} = \sum_{i=1}^{N} F_{\rm d,i} / V_{\rm cell} \tag{3}$$

where $F_{\rm d,i}$ is the force of the fluid on the *i*th TPB (including fluid drag force, resistance, lift force, additional mass force, and pressure gradient force), N.

Newton's second law describes the microscopic motion of the TPB in a horizontal wellbore, and the equation (Baldini et al., 2018; Wu and Sharma, 2019) for the translational motion of the TPB in a horizontal wellbore is

$$m_{\rm b} \frac{{\rm d}v_{\rm b}}{{\rm d}t} = m_{\rm b}g + F_{\rm P} + F_{\rm D} + F_{\rm S} + F_{\rm M} + F_{\rm VM}$$
 (4)

where m_b is the mass of the TPB, kg; v_b is the transportation speed of the TPB, m/s; F_p is the pressure gradient force due to the presence of a pressure gradient of the fluid in the horizontal wellbore, N; and F_D , F_S , F_M , and F_{VM} are the dragging force, shear lift, rotational lift, and additional mass force of the fluid on the TPB, N, respectively.

The equation (Wang et al., 2018; Ismail et al., 2021) for the rotational motion of the TPB is

$$I\frac{\mathrm{d}\omega_{\mathrm{b}}}{\mathrm{d}t} = \sum T_{\mathrm{c}} + T_{\mathrm{f}} \tag{5}$$

where I is the inertia tensor, kg m²; ω_b is the angular velocity of the TPB, rad/s; T_c is the torque due to the contact force between the ball and the ball, N m; and T_f is the torque due to the fluid shear, N m.

3. Model verification

Since the transportation of TPB in the horizontal wellbore is a complex process, it is essential to verify the accuracy of numerical simulation through visually physical experiments.

3.1. Verified by the TPB transportation state

Qu et al. (2024) conducted a series of TPB migration experiments in a horizontal, transparent pipe with several spiral holes. The TPB migration in the horizontal pipe at different times was recorded by a high-speed camera. A geometric model of the same size pipe with Qu's experiment (Qu et al., 2023, 2024) is used in our numerical simulation.

When the fluid flow rate is 1.4 m/s and the diameter of TPB is 9 mm, the TPB migration trajectory in the numerical simulation (see the sketch with ball trajectory in Fig. 1) is compared to the experimental result (see the picture in Fig. 1). The TPB is suspended until the end-top hole, which is basically consistent with the Qu's experiment (Qu et al., 2024) (see Fig. 1).

When the fluid flow rate is 0.75 m/s and the diameter of TPB is 12 mm, the TPB transport is no longer in a suspension state (see the picture in Fig. 2). The TPB moves closer to the bottom of the wellbore, which is also consistent with the Qu's experiment (Qu et al., 2024) (see Fig. 2).

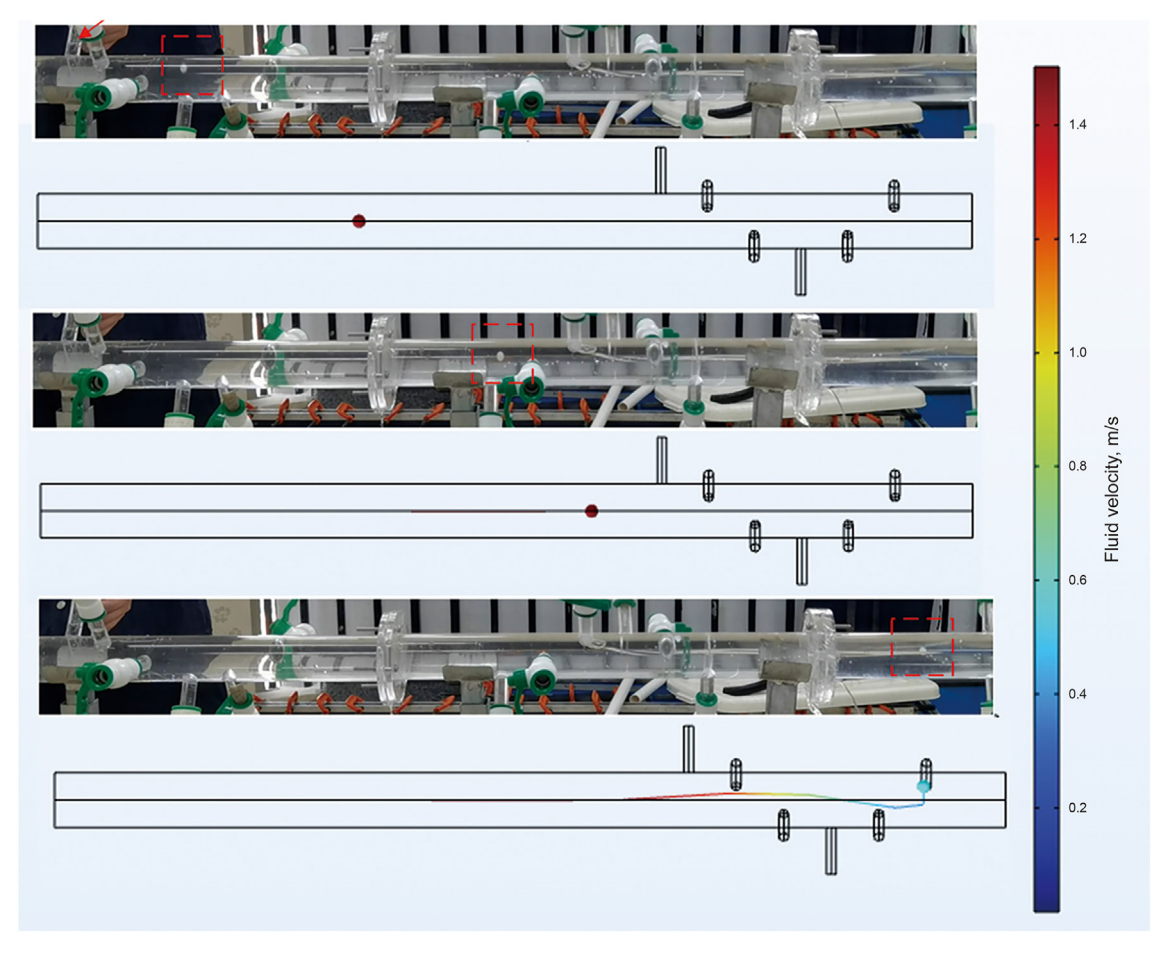


Fig. 1. Comparison of TPB transportation at $v_f = 1.4$ m/s (experimental results from Qu et al., 2024).

3.2. Verified by the threshold fluid velocity

To further verify the accuracy of the numerical simulation of TPB transportation, the threshold velocities for ball suspension under different conditions in the numerical simulation are compared with them in the physical experiment in this section. The threshold velocities for ball suspension in five cases with different ball densities and diameters were given in the Qu's experiments (Qu et al., 2024). The threshold velocities measured in this numerical simulation are 1.18, 1.75, 1.47, 1.54, and 1.46 m/s, respectively. The comparison between the Qu's experiment (Qu et al., 2024) and this numerical simulation is given in Fig. 3. The maximum relative error is 8.15%, and the average relative error is only 3.98%.

4. Example of a numerical simulation

The common casing size in horizontal well staged fracturing is selected, and a casing length of 1200 mm is taken as the simulated length. The perforation numbers P_1 , P_2 , P_3 , P_4 , P_5 , and P_6 are assigned from the borehole toe to the heel in the spiral perforation (Fig. 4).

In Fig. 4, the borehole heel is set up as the fluid and TPB inlet. The perforation outlet is set up as the pressure outlet, and the borehole toe is set up as the plugging point. The specific parameters are shown in Table 1.

Five major factors given in Table 2 affect the TPB migration and sealing behaviour.

The mesh division method adopts hydrodynamic alignment, coarsening the wellbore mesh, and refining the perforation mesh to ensure the mesh independence. The mesh division is illustrated in Fig. 5.

The model solution uses two-phase flow models, including the discrete model and continuous medium model. To simulate the behaviour of the discrete phase and track the TPBs' trajectory, the particle tracking module of COMSOL simulation software is utilized. To simulate fluid behaviour, the fluid flow module calculates velocity and pressure fields based on fluid dynamics. Finally, the model considers the interaction and coupling effects between the continuous phase and the two phases simultaneously and performs the model solving. The interaction and coupling effects between the continuous phase and the discrete phase are then considered simultaneously, and the model is solved accordingly. A flowchart of the TPB migration simulation is shown in Fig. 6.

When the model parameters use the initial values (see them in Table 2), the physical field of this model is solved in each time step, and the final solution is obtained via postprocessing. The trajectories of the TPBs at different times are then plotted in Fig. 7. The pressure streamline of the flow field is shown in Fig. 8.

In Fig. 7, the TPBs in the horizontal wellbore moved downwards due to gravity and were affected by various forces, such as drag force, pressure gradient force, lift force, and additional mass force, which caused translational and rotational movements in the horizontal and vertical directions, respectively. The plugging balls bounced back when they hit the wellbore wall until they reached

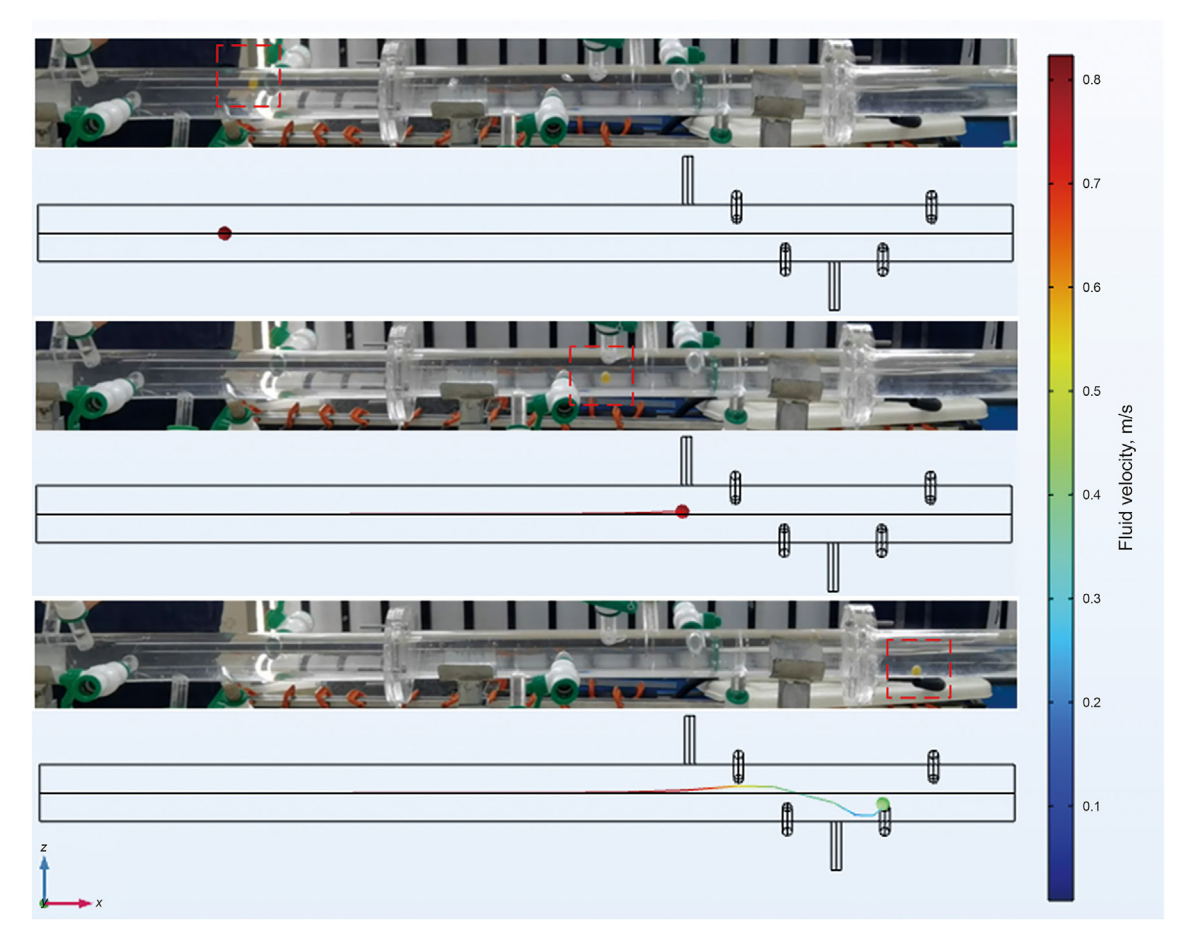


Fig. 2. Comparison of TPB transportation state at $v_f = 0.75$ m/s (experimental results from Qu et al., 2024).

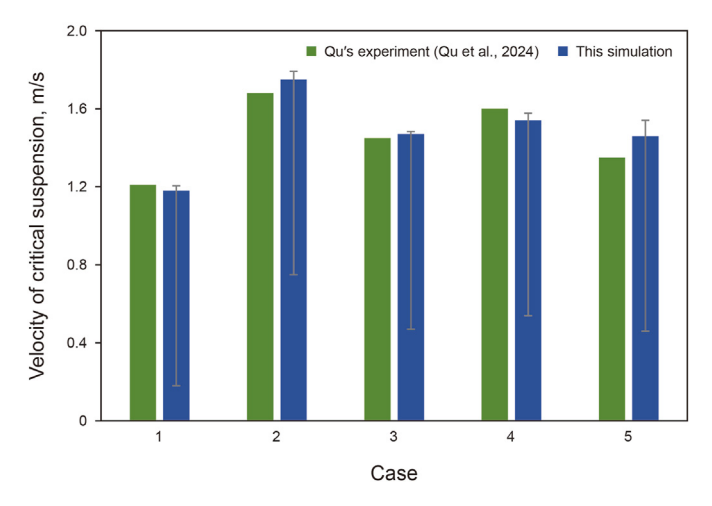


Fig. 3. Comparison of threshold velocity between the physical experiment and numerical simulation.

the perforation or the borehole toe. To observe the final position of the TPBs easily, their trajectories at the final time of the simulation in the perforation section are plotted in Fig. 9.

From Fig. 9, the TPBs were more inclined to block the perforations near the borehole toe (P_1 to P_4) when they were transported in the horizontal wellbore by gravity, drag force, pressure gradient force, and lift force. Comparing the four perforations, the TPBs were more inclined to block P_3 and P_4 , indicating that the TPBs were

more inclined to block perforations located in the middle of the horizontal wellbore towards the bottom under the initial conditions.

To improve the plugging efficiency of TPBs, the influence of five major factors (See in Table 2) on the sealing pattern of TPB transportation needs to be further explored in Section 5.

5. Analysis of influencing factors

The main factors affecting the sealing of ball transportation are the ball density, ball diameter, and ball number, as well as the injection rate and viscosity of the fracturing fluid. In this section, numerical simulations are performed using the single-variable method to analyse the influence of each factor on TPB sealing.

5.1. TPB density

Since the TPBs are affected by gravity in the horizontal wellbore and their diameter is set to 15 mm, we adjust the amount of gravity by only changing the density of the TPBs in this study. Assuming that the initial conditions of the model remain unchanged, the density of the TPBs is set to 800, 900, 1000, 1100, or 1200 kg/m 3 . The number of balls plugging at the perforation is given in Fig. 10.

As shown in Fig. 10, when the density of the TPBs was 800 kg/m^3 , no TPBs were present in central P_4 , P_3 or P_1 near the upper borehole toe. However, there were TPBs in P_6 and P_5 near the borehole heel. This outcome suggests that when the density of TPBs is lower than that of the fracturing fluid, the TPBs are affected by buoyancy forces and tend to block upper perforations near the

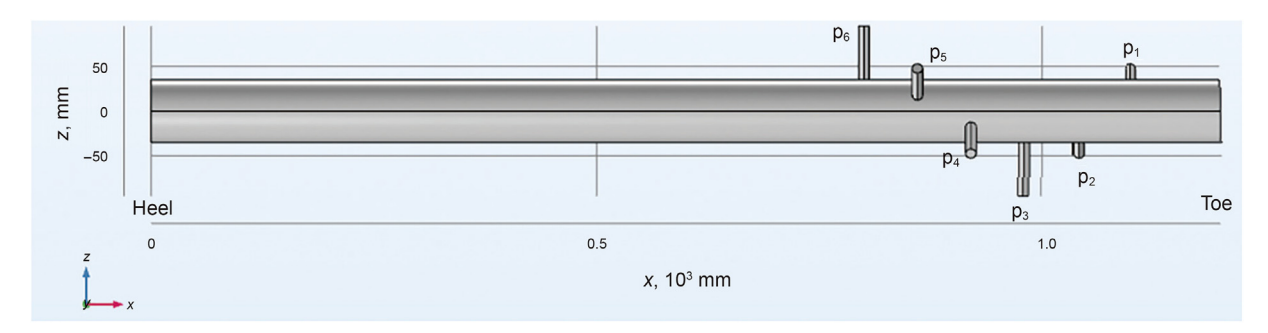


Fig. 4. 3D calculation model.

Table 1Geometric parameters of the 3D calculation model.

Outer diameter, mm	Inner diameter, mm	Phase angle, °	Perforation spacing, mm	Perforation diameter, mm	Density of the fracturing fluid, kg/m ³
88.9	73.0	60	60	12.0	1000

Table 2 Input data for the 3D calculation model.

Parameter	Initial value	Value
Injection rate of fracturing fluid, m ³ /min	5	0.5, 1.0, 1.5, 2.0, 2.5
Viscosity of fracturing fluid, mPa s	50	10, 20, 30, 40, 50
Diameter of TPBs, mm	15	12, 13, 14, 15, 16
Density of TPBs, kg/m ³	1000	800, 900, 1000, 1100, 1200
Number of TPBs	12	6, 9, 12, 15, 18

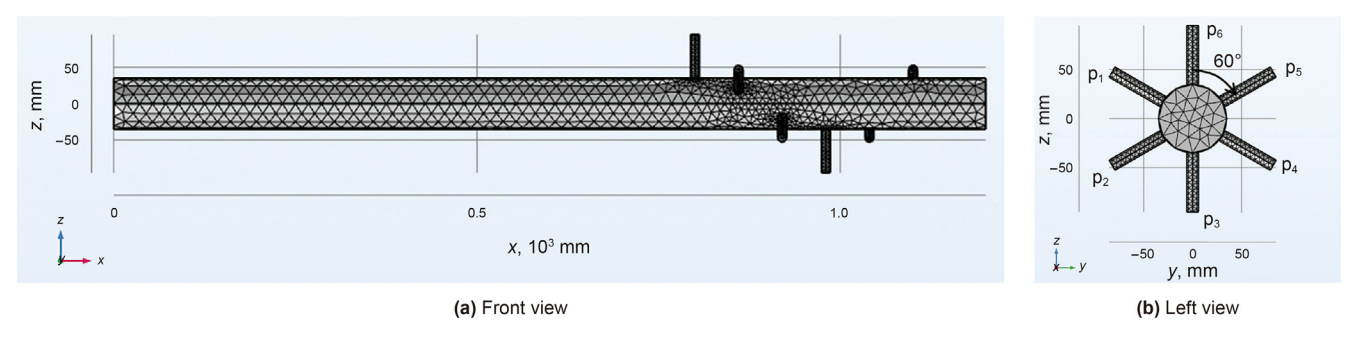


Fig. 5. Calculation model meshing.

borehole heel. When the density of the TPBs was increased to 900 kg/m³, P₄ and P₃ remained unplugged by TPBs, while P₅, P₂, and P₁ were plugged. This result indicates that when the density of the TPBs is 800 kg/m³ and that of the fracturing fluid is 1000 kg/m³, the TPBs tend to plug the perforation between P₆ and P₁. With increasing density of TPBs, the plugging efficiency of P₁ near the borehole toe improved. When the density of the TPBs was 1000 kg/ m³, perforations P₆, P₅, P₄, P₂, and P₁ were plugged by the TPBs, indicating that the plugging efficiency was greater. When the density of the TPBs was 1100 kg/m³, TPBs were absent from perforations P₆, P₅, and P₄ but present in perforations P₃, P₂, and P₁. This result indicates that if the density of the TPBs is greater than that of the fracturing fluid, then the TPBs tends to block the perforations near the borehole toe due to the influence of gravity. In addition, the perforations in the middle of the horizontal wellbore are more effective than those in the other locations in the downwards direction. When the density of the TPBs was 1200 kg/m³, perforations P₅, P₄, and P₂ were plugged, while the other perforations remained unplugged. This result indicates that when the

density of the TPBs is higher than that of the fracturing fluid $(1000 \ kg/m^3)$ and increases from 1100 to 1200 kg/m^3 , the TPBs tend to plug the perforations close to the borehole toe and downwards facing. For engineering purposes, using TPBs with mixed input density can be beneficial. Specifically, using TPBs with a density lower than that of the fracturing fluid will ensure better plugging efficiency near the borehole heel. Using TPBs with a density higher than that of the fracturing fluid will similarly improve the plugging efficiency near the borehole toe.

5.2. TPB diameter

To study the effect of the diameter of the TPBs on the transport plugging efficiency, we assumed that the initial conditions of the model remained unchanged and that the diameters of the TPBs were set to 12, 13, 14, 15, and 16 mm. The number of balls plugging at the perforations is given in Fig. 11.

As shown in Fig. 11, when the diameter of TPBs is 12 mm, there were no TPBs near the borehole heel in P_6 or P_5 . However, P_4 and P_3 ,

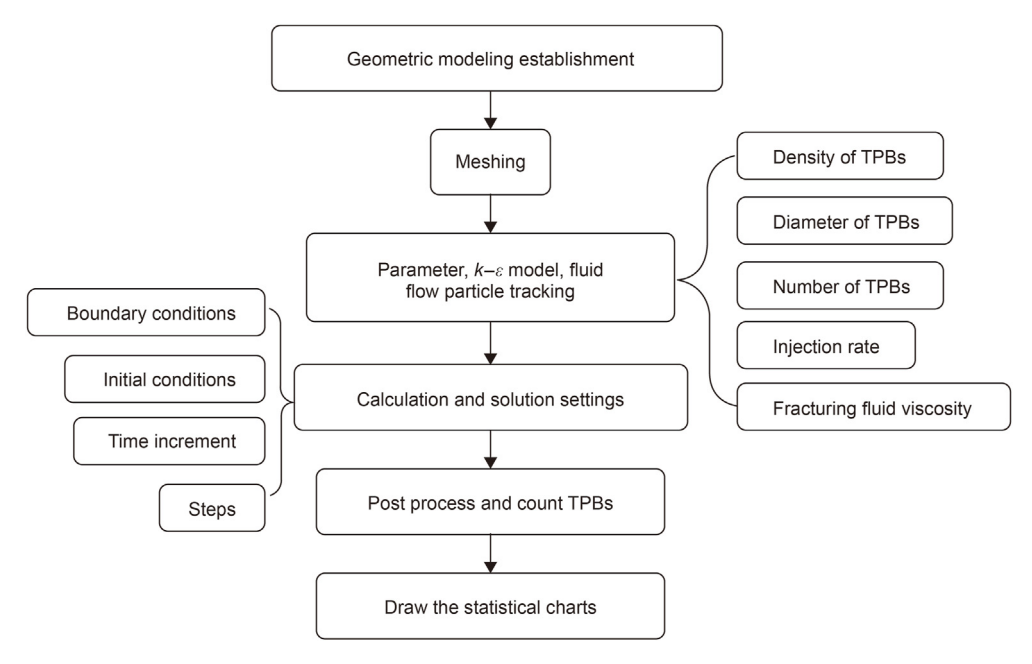


Fig. 6. Flowchart of the TPB migration simulation.

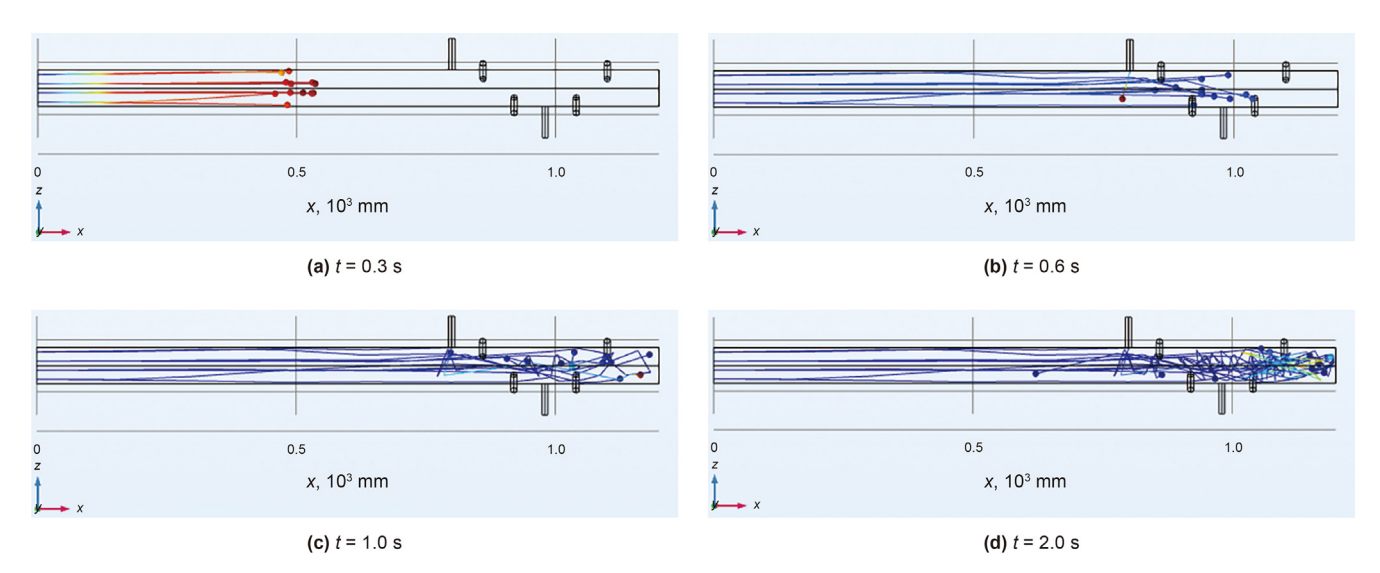


Fig. 7. Trajectories of the TPBs at different times.

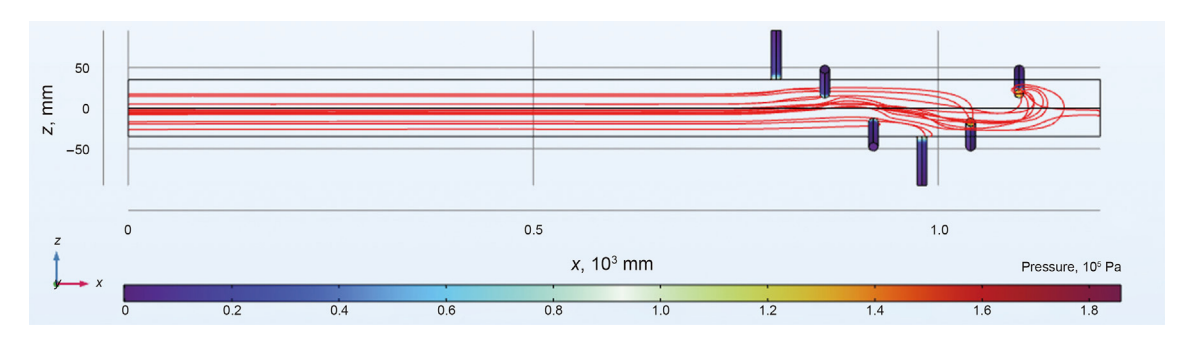


Fig. 8. Pressure streamline of the flow field of 12 TPBs.

which are in the central part of the perforation section, were plugged, as were P_2 and P_1 near the borehole toe. For the TPBs with

diameter of 13 and 14 mm, no TPBs were found in P_6 . However, for the TPBs with diameter of 15 and 16 mm, P_6 was plugged by TPBs.

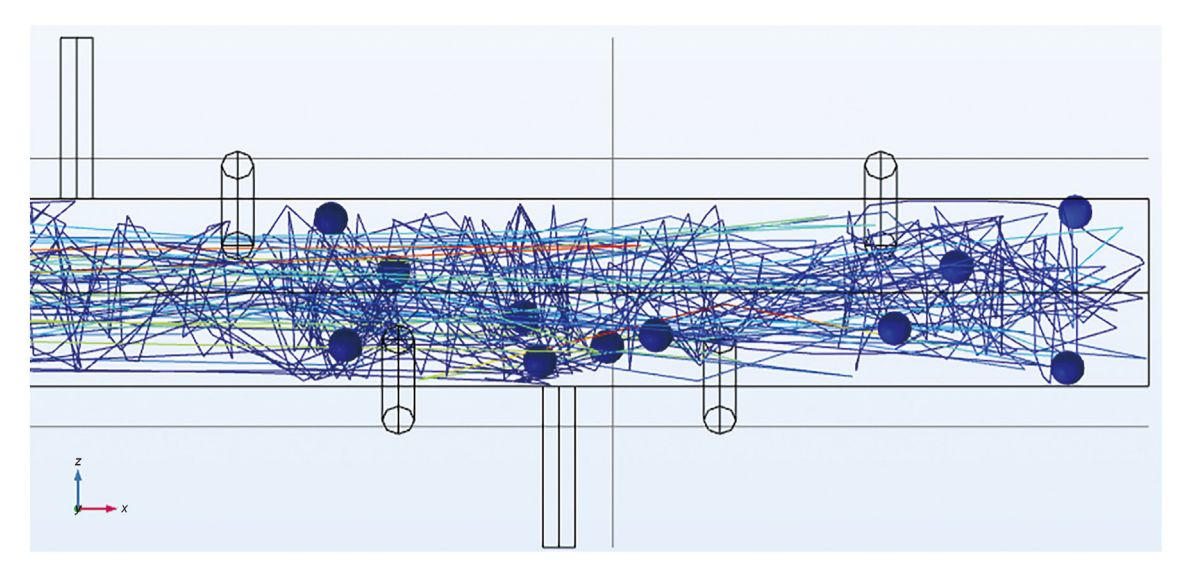


Fig. 9. Trajectory of the TPBs in the perforation section at final time.

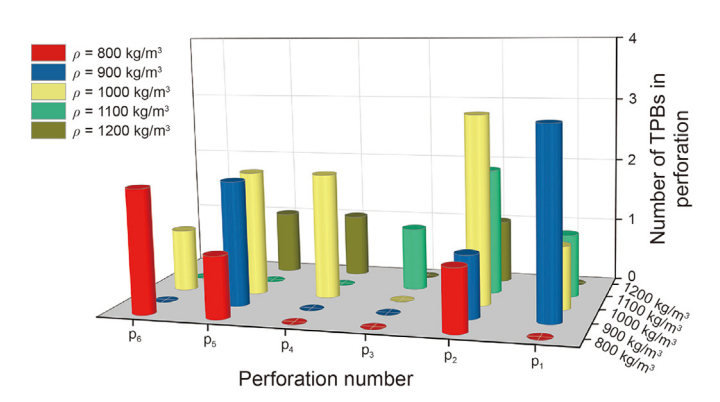


Fig. 10. Density of TPBs vs. number of TPBs in P_1-P_6 .

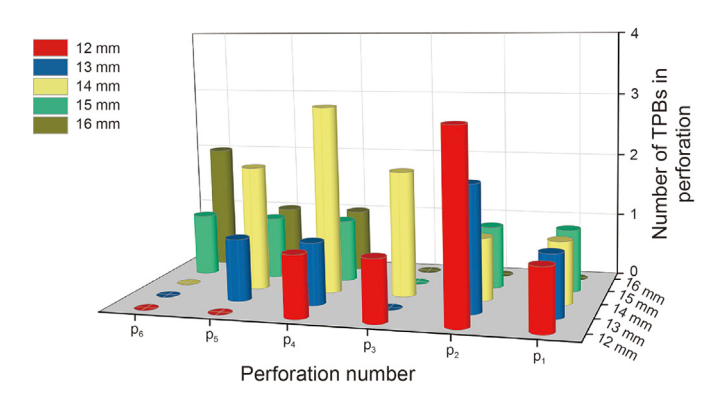


Fig. 11. Diameter of TPBs vs. number of TPBs in P_1-P_6 .

However, with a diameter of 16 mm, no TPBs were found in P_2 or P_1 near the borehole toe. The above phenomena show that when the diameter of the TPBs is small, the TPBs are easily carried and plugged in the middle and near the borehole toe in the horizontal well. As the diameter of the TPBs increases, it becomes easier for the TPBs to plug perforations near the borehole heel in the upper part due to the buoyant force. In brief, a smaller TPB diameter decreases the plugging efficiency near the borehole heel, while a larger diameter increases the plugging efficiency near the borehole

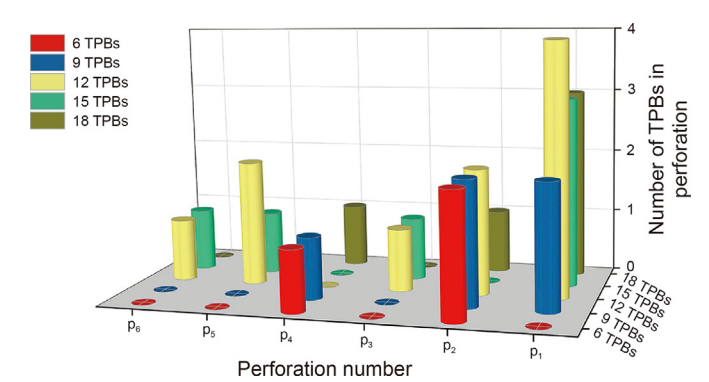


Fig. 12. Number of TPBs vs. the number of TPBs in P_1-P_6 .

heel. The plugging efficiency is greater when the diameter of TPBs is between 13 and 15 mm, and the plugging efficiency first increases and subsequently decreases within this interval. TPBs of diameter of 14 mm yield the highest plugging efficiency, indicating that a moderate diameter of TPBs substantially improves plugging efficiency. In other words, the plugging efficiency is greater when the diameter of TPBs is approximately 1.08—1.25 times the perforation diameter.

5.3. TPB number

In the study of the sealing law of TPB transportation, the TPB number is also an important factor. A few balls may not be able to achieve a better plugging effect, while many balls will increase its cost. This study aimed to determine the optimal number of TPBs needed to achieve the optimal plugging effect. Assuming that the initial conditions of the model remain unchanged, the number of TPBs is set to 6, 9, 12, 15, and 18. The number of balls plugging at the perforation is given in Fig. 12.

As shown in Fig. 12, when the number of perforations was equal to the number of TPBs, which was 6, only P_4 and P_2 were plugged with TPBs. This outcome suggests that when the number of TPBs is 6, the plugging efficiency is low, and no clear pattern emerges. When the number of TPBs was 9, TPBs were plugged in P_2 or P_1 but not P_6 or P_5 . This result indicates that with an increase in the number of TPBs, the TPBs are inclined to be carried and plug the

perforations near the borehole toe. When the number of TPBs was 12, P₆, P₅, P₃, P₂, and P₁ were plugged with TPBs. This result indicates that when the TPB number is twice the perforation number, the plugging efficiency is considerably greater than that for 6 TPBs. When the number of TPBs was 15, perforations P₆, P₅, P₃, and P₁ were plugged with TPBs. Compared with that of 6 TPBs, the plugging efficiency of the TPBs was considerably greater. However, compared with that of the 12 TPBs, the plugging efficiency decreased. Accordingly, when the TPBs reached twice the number of perforations, the TPBs tended to interact more with each other. This interaction led to their movement towards the borehole toe, which resulted in a decrease in plugging efficiency. When the number of TPBs was 18, only perforations P4, P2, and P1 were plugged by TPBs. This result indicates that the plugging efficiency decreases with an increase in the number of TPBs more than twice that of the perforations.

5.4. Injection rate of the fracturing fluid

In horizontal well ball-throwing for temporary plugging fracturing technology, the injection rate is an important parameter that affects TPB transportation and the plugging process. The position of the plugging ball can be controlled by changing the injection rate, which improves the plugging efficiency. Assuming that the initial conditions of the model remain unchanged, the injection rates are set to 0.5, 1.0, 1.5, 2.0, and 2.5 m³/min. The number of TPBs plugged at the perforation sites is given in Fig. 13.

Fig. 13 shows that when the injection rate was 0.5 m³/min, the P₆, P₅, P₄, P₃, P₂, and P₁ perforations had TPBs. The plugging efficiency was high, indicating that effective plugging could be achieved at this injection rate. When the injection rate was 1.0 m³/min, all the perforations had TPB plugging, and the total number of TPBs was equal to that when the injection rate was 0.5 m³/min. This result indicates that when the injection rate increases to 1.0 m³/ min, the plugging efficiency is still high. When the injection rate was 1.5 m³/min, P₆ and P₃ had no TPB plugging. This result indicates that as the injection rate increases, the TPBs migrate at a faster speed. Consequently, it becomes more difficult to plug perforations near the heel of a horizontal wellbore, while perforations near the borehole toe are easier to plug. When the injection rate was 2.0 m³/ min, except for P₃, the perforations had TPBs. This result indicates that the position of the TPBs can be controlled by adjusting the injection rate so that the P₆ perforation close to the upper part of the borehole heel can be blocked. This method of adjusting the injection rate can improve the plugging efficiency. When the injection rate was 2.5 m³/min, TPBs were not observed at P₆ or P₃, and the number of TPBs at P₁ increased. This result suggests that as the injection rate increases, it becomes more challenging to achieve

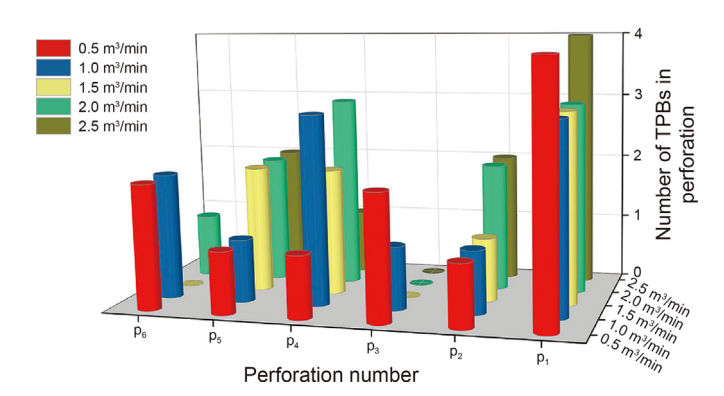


Fig. 13. Injection rate vs. number of TPBs in P_1-P_6 .

plugging at P_6 near the upper part of the borehole heel and P_3 located in the central part of the perforation section. To improve the plugging efficiency, the injection rate must be regulated to a moderate level.

5.5. Fracturing fluid viscosity

The fracturing fluid viscosity has an important effect on the transportation and plugging process of TPBs in horizontal wells. To study the effect of fracturing fluid viscosity on the TPB transportation and plugging process, the initial conditions of the model are unchanged. The fracturing fluid viscosity is set to 10, 20, 30, 40, and 50 mPa s. The number of balls plugging at the perforations is given in Fig. 14.

Fig. 14 shows that the viscosity of the fracturing fluid had a considerable effect on the plugging process during TPB transportation, especially at P₆, P₅, P₂, and P₁. Increasing the viscosity of the fracturing fluid increased the number of plugging balls plugged in P2 and P1 near the borehole toe and decreased the number of plugging balls plugged in P₆ and P₅ near the borehole heel. This outcome suggests that an increase in the viscosity of the fracturing fluid will increase the plugging efficiency of perforations near the borehole toe but decrease the plugging efficiency of perforations at the upper part near the borehole heel. P₄, located in the central part of the perforation section and having a phase angle of 120°, was plugged at each viscosity. This result indicates that the plugging efficiency of this perforation is high at all fracturing fluid viscosities in this area. In contrast, P3, located in the central part of the perforation section with a phase angle of 180°, had only a few TPBs plugged at all fracturing fluid viscosities. Upon comparison, it was found that perforations located in the central part of the perforation section and with a phase angle of 120° were more likely to be blocked.

6. Conclusions

The numerical simulation results of each group were comprehensively compared and analysed, the influence laws of the five major factors on the plugging properties of TPB transport were summarized, and the following conclusions and recommendations were drawn.

(1) Density of TPBs: When the density of the TPBs is lower than that of the fracturing fluid, the TPBs tend to plug the upper perforation. When the density of the TPBs is higher than that of the fracturing fluid, the TPBs tend to plug the lower perforation. When the density of the TPBs is close to that of the fracturing fluid, all the perforations have a better plugging effect. To enhance the plugging efficiency with a

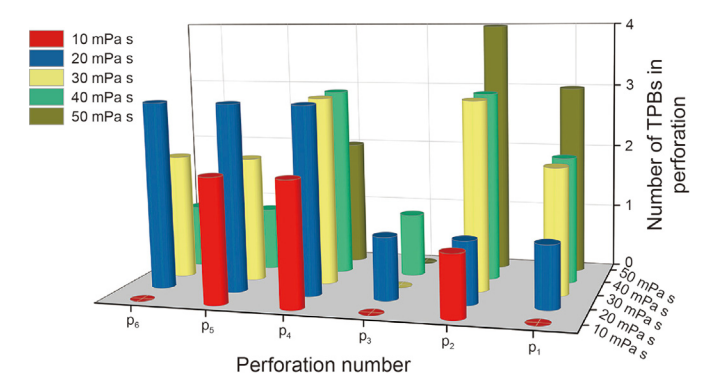


Fig. 14. Fracture fluid viscosity vs. number of TPBs in P_1-P_6 .

- specified ball diameter, it is suggested that the density of the TPBs closely matches that of the fracturing fluid. Moreover, a high plugging efficiency can be achieved by using TPBs with a mixed density.
- (2) Diameter of TPBs: This parameter has a substantial effect on the plugging efficiency of TPB transportation. The plugging efficiency of perforations near the borehole heel (P₅ and P₆) is low when the TPB diameter is 12 mm. The plugging efficiency of perforations near the borehole toe (P₁ and P₂) is low when the TPB diameter is 16 mm. The plugging efficiency is greater when the diameter of the TPB is approximately 1.08–1.25 times the perforation diameter.
- (3) Number of TPBs: If the parameters of horizontal well ball throwing for the temporary plugging fracturing process remain unchanged, changing the number of TPBs will affect the movement of the balls to plug the process. When the number of TPBs is equal to the number of perforations, the plugging efficiency is low. When the number of TPBs is increased to twice the number of perforations, the plugging efficiency will improve considerably. Increasing the number of TPBs increases the ball contact area with the perforations, which accelerates the process. However, with a larger number of TPBs, the plugging efficiency near the borehole toe will decrease. Moreover, when the number of TPBs is 3 times the number of perforations, the plugging efficiency decreases. Too many TPBs can easily push and carry each other to the borehole toe, thus decreasing the plugging efficiency.
- (4) Injection rate of fracturing fluid: In the case of a high injection rate in this study, it is difficult for the TPBs to effectively plug the upper perforation near the borehole heel (P₆), which leads to a lower plugging efficiency. In the case of a low injection rate, the TPBs can effectively plug the upper perforation near the borehole heel and realize the effective plugging of the other perforations, which ensures a higher plugging efficiency. In the ball-throwing temporary plugging fracturing process, a higher plugging efficiency can be achieved by reducing the injection rate appropriately.
- (5) Fracturing fluid viscosity: When the viscosity of fracturing fluid increases during ball throwing for temporary plugging fracturing, TPBs plug perforations near the borehole toe (P₁ and P₂) more easily but plug perforations near the borehole heel (P₅ and P₆) with more difficulty. However, the plugging efficiency of the middle perforations (P₃ and P₄) is almost unaffected by the viscosity of the fracturing fluid.

CRediT authorship contribution statement

Qing-Hai Hu: Writing — original draft, Validation, Methodology, Data curation. **Wan Cheng:** Supervision, Conceptualization. **Zun-Cha Wang:** Investigation, Formal analysis. **Yu-Zhao Shi:** Writing — original draft. **Guang-Liang Jia:** Writing — review & editing, Software, Resources, Project administration.

Declaration of competing interest

The authors declare that they have no known competing financial interests or personal relationships that could have appeared to influence the work reported in this paper.

Acknowledgements

This research was supported by the National Natural Science Foundation of China (No. 52074250).

References

- Barboza, B.R., Chen, B., Li, C., 2021. A review on proppant transport modelling. J. Petrol. Sci. Eng. 204, 108753. https://doi.org/10.1016/j.petrol.2021.1087.
- Baldini, M., Carlevaro, C., Pugnaloni, A., et al., 2018. Numerical simulation of proppant transport in a planar fracture. A study of perforation placement and injection strategy. Int. J. Multiphas. Flow 109, 207–218. https://doi.org/10.1016/i.jimultiphaseflow.2018.08.00.
- Baylocq, P., Fery, J.J., Parra, L., et al., 1999. Ball sealer diversion when fracturing long and multiple Triassic sand intervals on Alwyn Field, North Sea. In: SPE European Formation Damage Conference. https://doi.org/10.2118/54740-MS.
- Brown, R.W., Neill, G.H., Loper, R.G., 1963. Factors influencing optimum ball sealer performance. J. Petrol. Technol. 15 (4), 450–454. https://doi.org/10.2118/553-
- Cheng, W., Jiang, G., Xie, J., et al., 2019. A simulation study comparing the Texas twostep and the multistage consecutive fracturing method. Petrol. Sci. 16, 1121–1133. https://doi.org/10.1007/s12182-019-0323-9.
- Cheng, W., Lu, C., Feng, G., et al., 2021. Ball sealer tracking and seating of temporary plugging fracturing technology in the perforated casing of a horizontal well. Energy Explor. Exploit. 39 (6), 2045–2061. https://doi.org/10.1177/01445987211020414.
- Erbstoesser, S.R., 1980. Improved ball sealer diversion. J. Petrol. Technol. 32 (11), 1903–1910. https://doi.org/10.2118/8401-PA.
- Ismail, N.I., Kuang, S., et al., 2021. CFD-DEM study of particle-fluid flow and retention performance of sand screen. Powder Technol. 378, 410–420. https:// doi.org/10.1016/j.powtec.2020.10.012.
- Li, G., Wang, Y., He, R., et al., 2009. Numerical simulation of predicting and reducing solid particle erosion of solid-liquid two-phase flow in a choke. Petrol. Sci. 6, 91–97. https://doi.org/10.1007/s12182-009-0017-9.
- Li, H., 2017. Study on Migration Law of Degradable Ball Shaft and Plugging Technology in Perforation. Ph.D Dissertation. China University of Petroleum (Beijing) (in Chinese).
- Li, J., Dong, S., Hua, W., et al., 2020. Numerical simulation of temporarily plugging staged fracturing (TPSF) based on cohesive zone method. Comput. Geotech. 121, 103453. https://doi.org/10.1016/j.compgeo.2020.103453.
- Li, X., Chen, Z., Chaudhary, S.A., et al., 2005. An integrated transport model for ball-sealer diversion in vertical and horizontal wells. In: SPE Annual Technical Conference and Exhibition. https://doi.org/10.2118/96339-MS.
- Marchioli, C., Picciotto, M., Soldati, A., 2007. Influence of gravity and lift on particle velocity statistics and transfer rates in turbulent vertical channel flow. Int. J. Multiphas. Flow 33 (3), 227–251. https://doi.org/10.1016/j.ijimultiphaseflow.2006.09.005.
- Norouzi, H.R., Zarghami, R., Sotudeh-Gharebagh, R., et al., 2016. Coupled CFD-DEM Modeling: Formulation, Implementation and Application to Multiphase Flows. John Wiley & Sons.
- Nozaki, M., Zhu, D., Hill, A., 2013. Experimental and field data analyses of ball-sealer diversion. SPE Prod. Oper. 28 (3), 286–295. https://doi.org/10.2118/147632-PA.
- Olson, J.E., 2008. Multi-fracture propagation modeling: applications to hydraulic fracturing in shales and tight gas sands. In: The 42nd US Rock Mechanics Symposium, San Francisco. Paper Number: ARMA-08-327.
- Oberhofer, R., 2016. Application of ball-drop technology to improve efficiency and stimulation of limited entry completion systems. In: Abu Dhabi International Petroleum Exhibition & Conference. https://doi.org/10.2118/183427-MS.
- Qu, H., Chen, X., Hong, J., et al., 2023. Experimental and 3D numerical investigation on proppant distribution in a perforation cluster involving the artificial neural network prediction. SPE J. 28 (4), 1650–1675. https://doi.org/10.2118/214316-PA
- Qu, H., Liu, Y., Li, C., et al., 2024. Experimental and simulation investigation on ball-sealer transport and diversion performance aided by machine learning method. SPE J. 1–17. https://doi.org/10.2118/218010-PA.
- Rong, M., Xu, M., 2020. Mechanism of temporary blocking ball's transportation and blocking in shale gas horizontal wells. Sci. Technol. Eng. 20 (6), 2202–2208. CNKI:SUN:KXJS.0.2020-06-013. (In Chinese).
- Roussel, N.P., Mukul, M.S., 2011. Optimizing fracture spacing and sequencing in horizontal-well fracturing. SPE Prod. Oper. 26 (2), 173–184. https://doi.org/ 10.2118/127986-PA.
- Seale, R., Donaldson, J., Athans, J., 2006. Multistage fracturing system: improving operational efficiency and production. In: SPE Eastern Regional Meeting. https://doi.org/10.2118/104557-MS.
- Wang, D., Wang, X., Liu, G., et al., 2012. A new way of staged fracturing using ball sealers. SPE Prod. Oper. 27 (3), 278–283. https://doi.org/10.2118/140529-PA.
- Wang, S., Li, H., Wang, R., et al., 2018. Numerical simulation of flow behaviour of particles in a porous media based on CFD-DEM. J. Petrol. Sci. Eng. 171, 140–152. https://doi.org/10.1016/i.petrol.2018.07.039.
- Wu, C., Sharma, M., 2019. Modeling proppant transport through perforations in a horizontal wellbore. SPE J. 24 (4), 1777–1789. https://doi.org/10.2118/179117-PA.
- Xiong, C., Shi, Y., Zhou, F., et al., 2018a. Temporary plugging of deep oil and gas reservoirs to high-efficiency transformation and stimulation technology and application. Petrol. Explor. Dev. 45 (5), 888–893. https://doi.org/10.11698/ PED.2018.05.15 (in Chinese).
- Xiong, C., Shi, Y., Zhou, F., et al., 2018b. High-efficiency reservoir stimulation based on temporary plugging and diverting for deep reservoirs. Petrol. Explor. Dev. 45 (5), 948–954. https://doi.org/10.1016/S1876-3804(18)30098-3.

- Zeng, Y., Zhang, Xu, Zhang, B., 2015. Stress redistribution in multi-stage hydraulic fracturing of horizontal wells in shales. Petrol. Sci. 12, 628–635. https://doi.org/10.1007/s12182-015-0048-3.
- Zhang, R., Hou, B., Tan, P., et al., 2020. Hydraulic fracture propagation behaviour and diversion characteristic in shale formation by temporary plugging fracturing. J. Petrol. Sci. Eng. 190, 107063. https://doi.org/10.1016/j.petrol.2020.107063. Zhao, J., Chen, X., Li, Y., et al., 2016. Simulation of simultaneous propagation of
- Zhao, J., Chen, X., Li, Y., et al., 2016. Simulation of simultaneous propagation of multiple hydraulic fractures in horizontal wells. J. Petrol. Sci. Eng. 147, 788–800. https://doi.org/10.1016/j.petrol.2016.09.021.
- https://doi.org/10.1016/j.petrol.2016.09.021.

 Zhao, L., Chen, X., Zou, H., et al., 2020. A review of diverting agents for reservoir stimulation. J. Petrol. Sci. Eng. 187, 106734. https://doi.org/10.1016/

j.petrol.2019.106734.

- Zhou, H., Wu, X., Song, Z., et al., 2022. A review on mechanism and adaptive materials of temporary plugging agent for chemical diverting fracturing. J. Petrol. Sci. Eng. 212, 110256. https://doi.org/10.1016/j.petrol.2022.110256.
- Zhu, Y., Fang, X., Sun, X., et al., 2021. Development of degradable pre-formed particle gel (DPPG) as temporary plugging agent for petroleum drilling and production. Petrol. Sci. 18 (2), 479–494. https://doi.org/10.1007/s12182-020-00535-w.
- Zou, Y., Ma, X., Zhang, S., 2020. Numerical modeling of fracture propagation during temporary-plugging fracturing. SPE J. 25 (3), 1503—1522. https://doi.org/10.2118/199351-PA.